

Environmental Research Letters



LETTER

Earth system commitments due to delayed mitigation

OPEN ACCESS

RECEIVED

5 October 2015

REVISED

25 November 2015

ACCEPTED FOR PUBLICATION

7 December 2015

PUBLISHED

21 January 2016

Patrik L Pfister^{1,2} and Thomas F Stocker^{1,2}¹ Climate and Environmental Physics, Physics Institute, University of Bern, 3012 Bern, Switzerland² Oeschger Centre for Climate Change Research, University of Bern, 3012 Bern, SwitzerlandE-mail: pfister@climate.unibe.ch**Keywords:** climate change, ocean acidification, sea level rise, mitigation delay sensitivity, CO₂ emissions reduction, Earth system model, cumulative emissionsSupplementary material for this article is available [online](#)

Original content from this work may be used under the terms of the [Creative Commons Attribution 3.0 licence](#).

Any further distribution of this work must maintain attribution to the author(s) and the title of the work, journal citation and DOI.

**Abstract**

As long as global CO₂ emissions continue to increase annually, long-term committed Earth system changes grow much faster than current observations. A novel metric linking this future growth to policy decisions today is the mitigation delay sensitivity (MDS), but MDS estimates for Earth system variables other than peak temperature (ΔT_{\max}) are missing. Using an Earth System Model of Intermediate Complexity, we show that the current emission increase rate causes a ΔT_{\max} increase roughly 3–7.5 times as fast as observed warming, and a millennial steric sea level rise (SSLR) 7–25 times as fast as observed SSLR, depending on the achievable rate of emission reductions after the peak of emissions. These ranges are only slightly affected by the uncertainty range in equilibrium climate sensitivity, which is included in the above values. The extent of ocean acidification at the end of the century is also strongly dependent on the starting time and rate of emission reductions. The preservable surface ocean area with sufficient aragonite supersaturation for coral reef growth is diminished globally at an MDS of roughly 25%–80% per decade. A near-complete loss of this area becomes unavoidable if mitigation is delayed for a few years to decades. Also with respect to aragonite, 12%–18% of the Southern Ocean surface become undersaturated per decade, if emission reductions are delayed beyond 2015–2040. We conclude that the consequences of delaying global emission reductions are much better captured if the MDS of relevant Earth system variables is communicated in addition to current trends and total projected future changes.

1. Introduction

Global CO₂ emissions have been rising at a nearly exponential rate of roughly 2% per year over the past three decades (Boden *et al* 2013). Policy decisions in the next few decades will determine how long this rise continues, if its rate changes, and at what rate emissions can eventually be reduced. These near-term decisions will impact the Earth system and its climate for centuries to millennia (Weaver *et al* 2007, Plattner *et al* 2008, Friedlingstein *et al* 2011, Zickfeld *et al* 2013), due to the long atmospheric lifetime of CO₂ (Archer *et al* 2009, Joos *et al* 2013) and the inertia of the climate system. This can be illustrated using idealized CO₂ emission scenarios (Stocker 2013), in which global annual emissions continue to increase exponentially at a constant rate r up to a time t_1 when a

‘global mitigation scheme’ takes effect. After t_1 , annual emissions decrease exponentially at a constant rate s , which is limited by technological and economic feasibility (den Elzen *et al* 2007).

The cumulative carbon emissions C_{∞} from these or more sophisticated increase-to-decrease scenarios can be linked to future temperature increases using climate models, or using the linear relationship $\Delta T_{\max} = \beta_T C_{\infty}$ as a good approximation (Allen *et al* 2009, Matthews *et al* 2009, Steinacher and Joos 2015), where β_T is the peak response to cumulative emissions. This allows the estimate of the lowest achievable temperature target given an emissions reduction profile (Stocker 2013). Conversely, one can also estimate the necessary reduction profiles to achieve certain temperature targets such as the 2 °C target (Friedlingstein *et al* 2011, Rogelj *et al* 2011,

Peters *et al* 2013). Such estimates are evidently dependent on the starting year of emission reductions t_1 , leading to the important complementary question: what are the consequences of delaying mitigation?

In terms of economic cost, this question has been extensively explored (Bosetti *et al* 2009, Jakob *et al* 2012, Luderer *et al* 2013). These studies show that reaching certain climate targets becomes more expensive, and eventually unfeasible, while mitigation is delayed. In terms of Earth system commitments, however, quantitative estimates of the changes caused by delaying mitigation are sparse. Here, ‘Earth system commitments’ refers to future changes in the Earth system that are unavoidable based on the presently chosen emission pathway. Only for global mean temperature, estimates linking mitigation delays to additional commitments exist (Ramanathan 1988, Hare and Meinshausen 2006, Friedlingstein *et al* 2011, Allen and Stocker 2014). They were obtained from simple models under specific scenarios, and amount to roughly 0.1 °C–0.5 °C per decade of delay (evaluated at different times between AD 2100 and AD 3000). But limiting temperature changes alone may not be sufficient to meet the ultimate objective of the United Nations Framework Convention on Climate Change (UNFCCC), to prevent ‘dangerous anthropogenic interference with the climate system’ (Steinacher *et al* 2013).

The purpose of this study is to determine the additional commitments due to delayed mitigation for a range of policy-relevant quantities. These include ΔT_{\max} , the thermal expansion component of millennial sea level rise (SSLR), and two ocean acidification metrics. The latter are derived from the extent of sea surface areas that are either undersaturated or strongly supersaturated with respect to aragonite (Steinacher *et al* 2013). These areas are highly sensitive to CO₂ emissions and relevant for coral reefs (Kleypas *et al* 1999, Steinacher *et al* 2013, Pörtner *et al* 2014) and other shell-forming marine organisms (Orr *et al* 2005, Doney *et al* 2009, Pörtner *et al* 2014). Following Allen and Stocker (2014), we evaluate the mitigation delay sensitivities (MDSs) of these four quantities.

The MDS of an Earth system variable is defined as the rate of change in the commitment of that variable with changing t_1 (i.e., with delay in reducing CO₂ emissions), assuming a given emission pathway before and after t_1 . This is a generalization of the definition by Allen and Stocker (2014), who have estimated the MDS of ΔT_{\max} analytically using the linear relation $\Delta T_{\max} = \beta_T C_{\infty}$. However, for some other policy-relevant quantities, the MDS cannot be estimated analytically. For example, evaluating the spatiotemporal evolution of ocean acidification metrics requires a three-dimensional ocean biogeochemistry model. The model must be computationally efficient to explicitly simulate long-term changes for a large number of scenarios. For this purpose, we choose the Bern3D-LPX model (Ritz *et al* 2011, Stocker *et al* 2013), an Earth

system model of intermediate complexity (EMIC). We examine the dependence of the MDS on the rate of increase (r) and subsequent decrease (s) in annual emissions. The influence of the equilibrium climate sensitivity (ECS) (IPCC 2013) is also investigated.

This paper is organized as follows. The model and experimental design are described in section 2, along with the Earth system variables that are analyzed. The results are presented in section 3 and discussed in section 4. Section 5 concludes.

2. Methods

We employ the Bern3D-LPX EMIC to evaluate the MDS of four policy-relevant Earth system variables (section 2.2).

2.1. Model description and experimental design

The Bern3D is a three-dimensional frictional geostrophic balance ocean model (Müller *et al* 2006) with a prognostic biogeochemistry component (Tschumi *et al* 2008) and a sea-ice component, coupled to a single-layer energy and moisture balance model of the atmosphere (Ritz *et al* 2011). We use an updated model version (Roth *et al* 2014) with improved high-latitude resolution, with a total of 41 × 40 horizontal cells (figure 1) and 32 depth levels (supplementary figure 7). The Bern3D model is coupled to a simplified version of the LPX-Bern dynamic vegetation model (Stocker *et al* 2013), which does not include peatlands, dynamic nitrogen or land use changes. This is sufficient for simulating the idealized CO₂ emission scenarios, which do not include land use and non-CO₂ forcings, and for our analysis which focuses on ocean and atmosphere variables. We do not include non-CO₂ forcings such as short-lived climate pollutants in our simulations, because these have a much smaller effect on long-term climate and ocean acidification than CO₂ (Caldeira and Kasting 1993, Bowerman *et al* 2013, Allen and Stocker 2014).

To assess the influence of the uncertainty in model response, three model versions with ECSs of 1.5 °C, 3.0 °C and 4.5 °C have been constructed, corresponding to the IPCC uncertainty range in ECS (IPCC 2013). The model is tuned to these ECS values by separate 2 × CO₂ equilibrium experiments using a simple feedback parameter λ . In these experiments, CO₂ concentrations are doubled from preindustrial and then kept constant for 5000 years. A term $\lambda \Delta T(t)$ in the global energy balance accounts for unresolved feedbacks (Ritz *et al* 2011), and λ is varied. By fitting the simulated ΔT after 5000 years to the prescribed λ values, we obtain a polynomial relation between λ and ECS, where λ values of −2.20, −0.70 and −0.12 Wm^{−2} K^{−1} correspond to ECSs of 1.5 °C, 3.0 °C and 4.5 °C. Only results from the simulations with an ECS of 3.0 °C are shown in the figures.

Corresponding figures for the other values are provided in the supplementary material.

Following a preindustrial spinup of the coupled Bern3D-LPX, each of the three model versions is forced with historical (AD 1750–2013) atmospheric CO₂ concentration data (Etheridge *et al* 1996, Siegenthaler *et al* 2005, Dlugokencky *et al* 2015). Other forcings are kept constant at preindustrial level. The total carbon uptake simulated by the model up to 2011 (488–533 GtC for high to low ECS) is on the lower end of the IPCC (2013) estimates of 555 (470 to 640) GtC. This is due to the rather low carbon uptake of the LPX-Bern model (103–142 GtC in our coupled simulations), while the ocean uptake of the Bern3D model (146–151 GtC) is in good agreement with IPCC estimates. The ECS-dependence of historical carbon uptake is mainly due to the temperature sensitivity of the land biosphere.

Following the historical concentration-driven simulations, the model is run up to AD 3000 and forced by idealized CO₂-only emission scenarios following Stocker (2013):

$$E(t) = \begin{cases} E_0 \cdot e^{r(t-t_0)} & t_0 < t \leq t_1 \\ E_0 \cdot e^{r(t_1-t_0)} \cdot e^{-s(t-t_1)} & t > t_1, \end{cases} \quad (1)$$

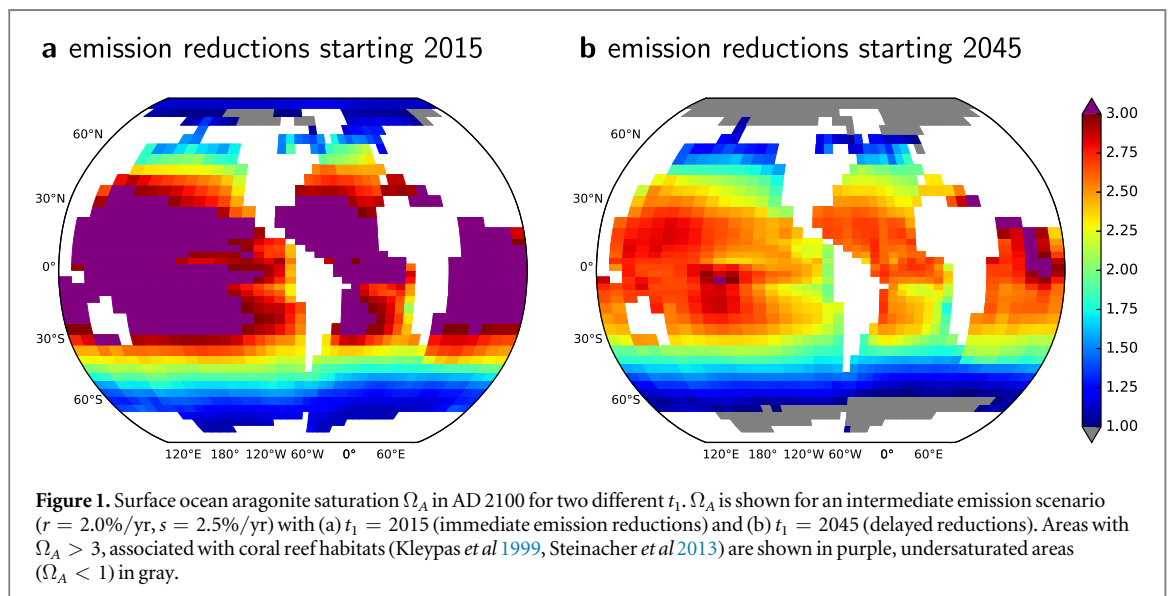
where $t_0 = 2013$ and $E_0 = E(t_0) = 9.86$ GtC (Boden *et al* 2013). Exponential fits of recent fossil fuel emission data (Boden *et al* 2013) yield an average increase rate r of 2.0%/yr for the 30 year period 1984–2013, and 2.6%/yr for the last decade 2004–2013. Estimates from economic models suggest that reduction rates s above 5%/yr are probably not feasible (den Elzen *et al* 2007). Therefore, the scenario parameters are varied as follows: r from 0%/yr (constant emissions up to t_1) to 4%/yr, and s from 0.5%/yr to 5%/yr, both in steps of 0.5%/yr. To diagnose MDS values valid for three decades, we vary t_1 from 2015 to 2045 in 13 non-equidistant steps (2015, 2018, 2020, 2023, etc), for each combination (r, s). This results in 1170 different idealized scenarios,

and a total of 3510 model simulations accounting for the three ECSs selected.

2.2. Earth system variables and MDS diagnosis

Two physical Earth system variables are analyzed, namely ΔT_{\max} and near-equilibrium SSLR. The time when ΔT_{\max} is reached generally increases with increasing C_{∞} and mostly ranges between roughly 40 and 600 years after present, consistent with Zickfeld and Herrington (2015). Only in some simulations with the highest ECS, there is still a slight warming after 1000 years, in which case ΔT_{\max} is evaluated at the end of the model run (AD 3000). SSLR is always evaluated in AD 3000. Although the ocean is not fully equilibrated at that time for some scenarios (supplementary figure 7), this provides a reasonable estimate of near-equilibrium SSLR. We prolonged the one model simulation forced by the highest emission scenario and found that SSLR(3000) reaches about 80% of equilibrium SSLR. For lower emission scenarios, the ocean in AD 3000 is probably even closer to equilibration. For the SSLR computation, the pressure-independent model density is adjusted assuming hydrostatic balance and using a pressure-dependent equation of state (simplified from UNESCO 1981) with the model ocean temperature and salinity. While this pressure adjustment only has a minor effect on short timescales, it becomes very relevant for longer timescales, when temperature changes reach the deep ocean where the pressure and its effect on density are larger. In AD 3000, the adjustment increases SSLR estimates by roughly 30%–90% (depending on ECS and scenario), indicating that SSLR is strongly underestimated if compressibility is neglected.

In addition, we explore two biogeochemical variables derived from the saturation state of aragonite in the surface ocean (Ω_A , figure 1), which is an important indicator of ocean acidification (Doney *et al* 2009, Pörtner *et al* 2014). Following Steinacher *et al* (2013),



we evaluate Ω_A changes in terms of surface area fractions. The first is the fraction A_{SO} of the Southern Ocean surface area south of 50° S that becomes undersaturated with respect to aragonite ($\Omega_A < 1$, gray in figure 1), thereby becoming corrosive to aragonitic shells of marine organisms (Orr *et al* 2005, Doney *et al* 2009, Pörtner *et al* 2014). The second is the fractional loss $L_{\Omega>3}$ of the global surface ocean area with more than threefold supersaturation ($\Omega_A > 3$, purple in figure 1), a relevant metric for coral reef habitats (Kleypas *et al* 1999, Steinacher *et al* 2013). Both fractions are evaluated at the end of the century (AD 2100). $L_{\Omega>3}$ is calculated as an additional loss commitment due to delaying mitigation, with respect to the preservable $\Omega_A > 3$ area for immediately starting emission reductions (figure 1(a)). This choice and its implications for the MDS are explained at the end of this section. For example, with emission reductions starting in 2015 at an intermediate s (figure 1(a)), $L_{\Omega>3}$ is 0% by definition and A_{SO} is also 0%, because aragonite undersaturation in the Southern Ocean is entirely mitigated. If reductions are delayed until 2045 (figure 1(b)), $L_{\Omega>3}$ is 96% of the area in figure 1(a), and A_{SO} is 25% of the area south of 50° S.

The MDS of each variable V is diagnosed from a least-squares linear fit of the simulated $V(t_1)$ on t_1 (figure 2). Each dot in figure 2 represents a single model simulation forced by an emission scenario uniquely identified by its parameters (r, s, t_1) . $MDS(V)$ is the slope of the linear fit, i.e., $MDS(V) = \Delta V / \Delta t_1$ (given in the figure legend). This diagnosis yields an average MDS over the investigated t_1 -interval, which is three decades for ΔT_{max} and SSLR. The t_1 -interval is shorter for A_{SO} and $L_{\Omega>3}$: for A_{SO} , it spans from the first t_1 causing $A_{SO} > 0$ to 2045; for $L_{\Omega>3}$, from 2015 to the first t_1 causing a near-complete loss of $\Omega_A > 3$ areas, as elaborated in the paragraph below. An MDS fit is not obtained if there are less than three t_1 -steps within this interval (white regions in figure 4). Note that this average MDS is also a reasonable approximation for instantaneous MDS, because the t_1 -dependence of all $V(t_1)$ is close to linear within the t_1 -interval ($R^2 > 0.95$ for most parameters).

Given an achievable reduction rate s , the maximum preservable $\Omega_A > 3$ area is obtained by immediately starting emission reductions (figure 1(a)). This area is chosen as the baseline $L_{\Omega>3} = 0$. $MDS(L_{\Omega>3})$ therefore indicates what part of the preservable area is lost due to delaying mitigation. Consequently, $MDS(L_{\Omega>3})$ deviates from the other MDS definitions in that the percentages for different s do not correspond to the same absolute area losses, because they scale with this scenario-dependent baseline. Based on the assumption that policy options are limited to t_1 for a given s , and thus to preserving an $\Omega_A > 3$ area between this baseline and zero, we consider this more relevant than a constant baseline (e.g., preindustrial $\Omega_A > 3$ areas). Most notably, this MDS definition contains information on how much delay would cause a near-complete

loss of global $\Omega_A > 3$ areas. We speak of a near-complete loss if less than 5% of preindustrial $\Omega_A > 3$ areas remain by 2100 (e.g., figure 1(b)). For the MDS diagnosis, losses are only fitted up to this value, because further losses are increasingly nonlinear with both cumulative emissions and t_1 (figure 2(d)). This indicates that the last remaining 5% of the $\Omega_A > 3$ areas are more resilient to further emissions, which may be a model-specific feature. These cells, located chiefly in the Indian Ocean, start from a particularly strong undersaturation at preindustrial times ($\Omega_A > 4.5$) and therefore require more emissions to cross the $\Omega_A = 3$ threshold. According to our definition, an $MDS(L_{\Omega>3})$ of 50%/decade thus indicates that a delay of two decades would cause a near-complete loss, for example.

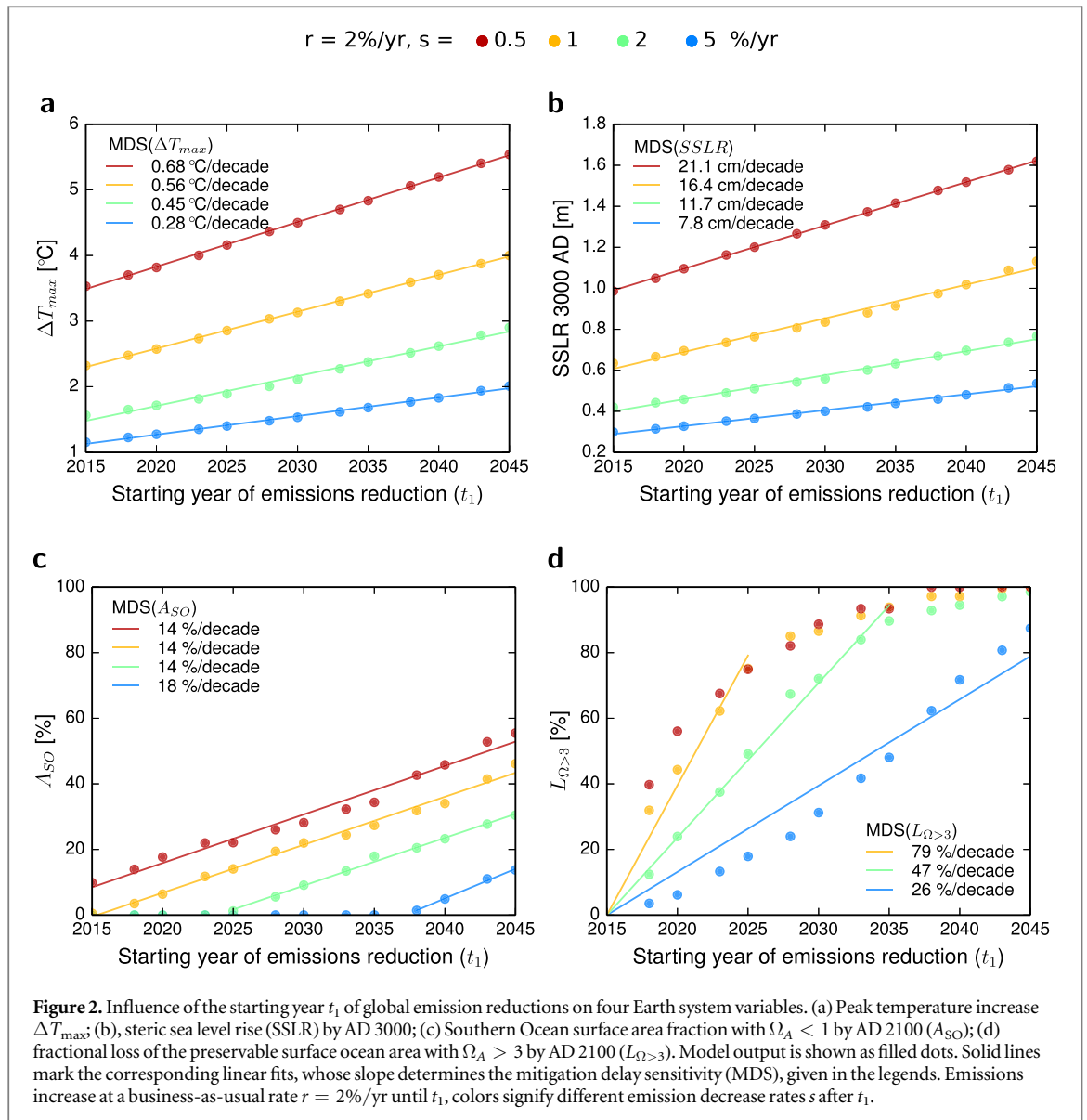
3. Results

3.1. MDS of physical variables

Firstly, projected changes in the physical variables ΔT_{max} and SSLR are presented. In agreement with other models and analytical considerations (Allen *et al* 2009, Matthews *et al* 2009, Williams *et al* 2012, Allen and Stocker 2014), these are mainly dependent on C_{∞} , which is determined by the scenario parameters r, s and t_1 (section 2.1). In figures 2(a) and (b), we focus on a business-as-usual increase rate $r = 2\%/yr$ to analyze the influence of t_1 for various s . Note that these figures contain much information beyond our MDS analysis. For example, figure 2(a) shows that the lowest achievable temperature target is strongly affected by the choice of s , or which (s, t_1) combinations are consistent with meeting the 2°C target according to our model. As these topics have been extensively covered in the recent literature (Friedlingstein *et al* 2011, Rogelj *et al* 2011, Peters *et al* 2013, Stocker 2013), we focus on describing the additional commitments due to delay in emission reductions, quantified by the MDS (section 2.2).

The MDSs of ΔT_{max} and SSLR increase substantially for smaller reduction rates s (figures 2(a) and (b)). With an intermediate ECS, they are estimated at roughly $0.3\text{--}0.7^\circ\text{C}/\text{decade}$ for ΔT_{max} and $8\text{--}21\text{ cm}/\text{decade}$ for SSLR by AD 3000, for s ranging from $5\%/yr$ down to $0.5\%/yr$. To better understand the significance of these numbers, they can be compared to the observed rates of warming and SSLR over the last few decades. This is done in table 1, which lists the factors between MDSs and model-diagnosed historical rates, along with related quantities as described in the following.

Model-diagnosed historical warming and SSLR rates are comparable to IPCC observed rates (table 1 and footnotes). To enable this comparison, two different time frames are chosen for the diagnosis (1951–2012 for warming and 1970–2011 for SSLR). Historical warming rates in the Bern3D-LPX (0.05 to $0.12^\circ\text{C}/\text{decade}$) are somewhat lower than observed



rates (0.08–0.14 °C/decade). This is because non- CO_2 forcings, which are overall positive over the historical period (IPCC 2013), are not included in our historical simulations. Nevertheless, the model-diagnosed historical rates are used for the comparison with the MDS, mainly because the IPCC uncertainty range does not uniquely correspond to the ECS uncertainty. Using the IPCC range regardless would result in slightly lower factors in the case of temperature. In the case of SSLR, there would be no difference, as the Bern3D-LPX range corresponding to the ECS uncertainty (0.49–1.13 cm/decade) is in very close agreement with the IPCC uncertainty range (0.5–1.1 cm/decade). While a somewhat lower rate would be expected due to the lack of non- CO_2 forcings, the median CMIP5 rate including these forcings (0.96 cm/decade) is still higher than our intermediate ECS rate (0.84 cm/decade). Also, the projected SSLR (measured by β_{SSLR}) is consistent with estimates by Williams *et al* (2012) (supplementary section 1.1).

As long as emission reductions are delayed, peak committed warming and millennial SSLR increase much faster than observed warming and SSLR (table 1). While the absolute $\text{MDS}(\Delta T_{max})$ and $\text{MDS}(\text{SSLR})$ values scale with ECS, the factors between MDS and historical rates are less strongly affected by the ECS. This is because the historical rates also scale with ECS (see previous paragraph). Nevertheless, the factors increase with increasing ECS because the present-day realized warming fraction (Frölicher and Paynter 2015) is lower in model versions with higher ECS. Here, the realized warming fraction is defined as $T(2013)/T_{eq}(2013)$, where $T_{eq}(2013)$ is the equilibrium temperature corresponding to the transient atmospheric CO_2 concentration. T_{eq} solely depends on the prescribed concentration and ECS, but the three model versions produce different $T(2013)$, resulting in realized warming fractions of 49%–66% (high to low ECS). The maximum factor increases less strongly than the minimum factor, and even decreases

Table 1. Simulated temperature and SSLR changes for different ECSs. Rates of change in projected peak temperature and millennial SSLR while emission reductions are delayed (MDS(ΔT_{\max}) and MDS(SSLR)) are compared to simulated historical rates. MDSs are several times larger than historical rates, as indicated by the factors in the last column. Ranges in MDSs and factors correspond to the simulated range of emission reduction rates s , from 5%/yr down to 0.5%/yr. The proportionality factors β_T and β_{SSLR} for the relations $\Delta T_{\max} = \beta_T C_{\infty}$ and $\text{SSLR}(3000) = \beta_{\text{SSLR}} C_{\infty}$ are diagnosed from all model scenarios with $C_{\infty} < 2$ TtC (supplementary section 1.1).

ECS (°C)	β_T (°C/TtC)	hist. rate ^a (°C/decade)	MDS(ΔT_{\max}) (°C/decade)	Factor
1.5	0.76	0.05	0.15–0.39	2.8–7.2
3.0	1.51	0.09	0.28–0.68	3.1–7.5
4.5	2.72	0.12	0.58–0.85	4.9–7.2
ECS (°C)	β_{SSLR} (cm/TtC)	hist. rate ^b (cm/decade)	MDS(SSLR) (cm/decade)	Factor
1.5	18	0.49	3.4–10.1	6.9–20.6
3.0	40	0.84	7.8–21.1	9.3–25.1
4.5	78	1.13	15.5–23.6	13.7–20.9

^a Simulated 1951–2012 average rate; to be compared with IPCC 1951–2012 observed rate of 0.12 [0.08–0.14] °C per decade (IPCC 2013).

^b Simulated 1971–2010 average rate; to be compared with IPCC 1971–2010 observed rate of 0.8 [0.5–1.1] cm per decade or the corresponding CMIP5 rate of 0.96 [0.51–1.41] cm per decade (Church *et al* 2013).

in the highest ECS model version, indicating that there is a counteracting effect. This effect is the increasing nonlinearity of the $\Delta T_{\max}/C_{\infty}$ relationship at high C_{∞} with increasing ECS (supplementary figure 5). Both effects may possibly be model-specific, or caused by the tuning of the ECS using a feedback parameter.

Overall however, the range of factors for the considered s range is not much different whether only the medium ECS or all ECS are considered. Including both the ECS uncertainty and the range of achievable s , we summarize: ΔT_{\max} increases roughly 3–7.5 times as fast as observed warming, and near-equilibrium SSLR increases 7–25 times as fast as observed SSLR.

How do these MDS estimates change if r deviates from the business-as-usual $r = 2\%/yr$ before emissions start to decrease? For such considerations, r should be viewed as an average increase rate, which is always lower than the peak increase rate in reality, because the transition to decreasing emissions cannot be as sharp as in the idealized scenarios. On the other hand, it is possible that r increases in the near future before approaching the transition. Therefore, we consider r values between 0%/yr (constant emissions up to t_1) and 4%/yr (double the 1984–2013 rate). Figure 3 shows MDS(ΔT_{\max}) and MDS(SSLR) for this r -range along with the previously considered s -range. Both MDSs scale with r for all s . They increase most rapidly with increasing r if s is low, however not quite as rapidly as analytical estimates suggest (supplementary

section 1). In line with increasing changes in cumulative emissions, the s -dependence of MDS(ΔT_{\max}) and MDS(SSLR) increases with increasing r . For comparison, figure 3(b) also shows the MDS of SSLR by AD 2100 (dashed contours), which is much lower than the near-equilibrium MDS(SSLR) (see also supplementary figure 7). Considering $r = 2\%/yr$, it amounts to 1.9–2.4 cm/decade depending on s , which is still more than twice as fast as observed SSLR. In contrast to the MDS of near-equilibrium SSLR, this short-term MDS increases with s , because the difference in cumulative emissions up to 2100 caused by delaying t_1 is larger for large s .

3.2. MDS of ocean acidification metrics

Returning to figures 2(c) and (d), we next present the projected changes in the ocean acidification metrics A_{SO} and $L_{\Omega > 3}$ for a business-as-usual emission increase rate $r = 2\%/yr$. These results are summarized for all model versions with different ECSs in table 2.

Partial aragonite undersaturation of the Southern Ocean surface in AD 2100 can be avoided with sufficiently early and stringent mitigation. Undersaturation ($A_{\text{SO}} > 0\%$) only occurs if a threshold in cumulative emissions up to 2100 is exceeded. In our model, this threshold ranges from roughly 1.0–1.2 TtC for high to low ECS, due to differences in carbon uptake caused by climate-carbon cycle feedbacks (Plattner *et al* 2001, Friedlingstein *et al* 2014). For fixed parameters r and s , this corresponds to a threshold delay in emission reductions, after which the MDS of A_{SO} is evaluated. The threshold delay strongly depends on s (figure 2(c)). For $s > 1\%/yr$, undersaturation can be entirely avoided if mitigation starts early enough. In contrast to the threshold delay, MDS(A_{SO}) is nearly independent of s and ECS. It amounts to 12%–18%/decade, indicating that roughly one sixth of the ocean surface becomes undersaturated per decade of mitigation delay, once the threshold delay is exceeded.

Further loss of some $\Omega_A > 3$ areas is unavoidable with $s \leq 5\%/yr$, but may be reduced by early mitigation. If CO_2 emission reductions were to start immediately, roughly 10%–75% of the preindustrial $\Omega_A > 3$ area could be preserved at the end of the century, depending on the achievable s (table 2 and supplementary figure 8(a)). This maximum preservable area defines the baseline for the further loss $L_{\Omega > 3}$ due to delay in emission reductions (section 2.2). Such delay increases the loss of $\Omega_A > 3$ areas substantially (figure 2(c) and supplementary figures 8(b) and (c)). This is quantified by the MDS($L_{\Omega > 3}$), indicating that the remaining $\Omega_A > 3$ area in AD 2100 shrinks rapidly by roughly 25%–80% per decade of delay (for $s \geq 1\%/yr$). The s -dependence of MDS($L_{\Omega > 3}$) mainly stems from its s -dependent baseline: The absolute area loss is only slightly s -dependent, but this absolute area

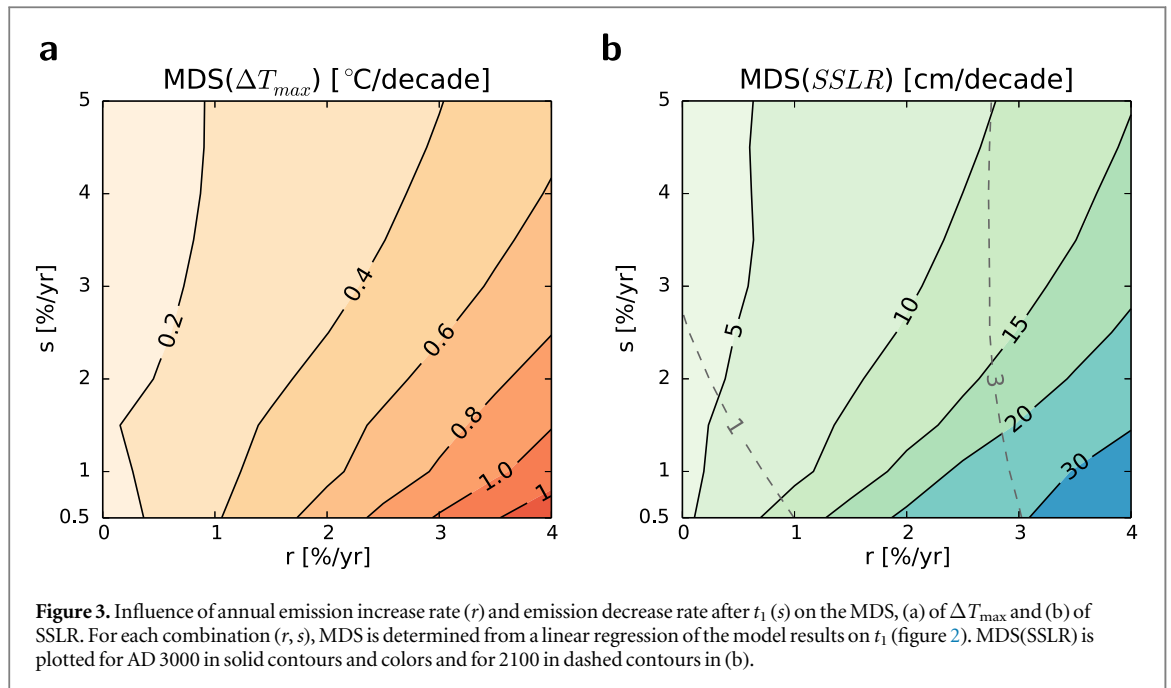


Table 2. Simulated changes in ocean acidification metrics projected for the end of the century, with different ECSs. $L_{\Omega > 3}$ is the fractional loss of preservable $\Omega_A > 3$ areas, and A_{SO} the fraction of the Southern Ocean surface where $\Omega_A < 0$ (see text). MDSs for both metrics are listed, along with their different kinds of baselines (see footnotes a and b). Ranges correspond to the simulated range of emission reduction rates s , from 5%/yr down to 0.5%/yr.

ECS (°C)	Threshold delay ^a (yr AD)	MDS(A_{SO}) (%/decade)
1.5	<2015–2040	15–18
3.0	<2015–2038	14–18
4.5	<2015–2033	12–15
ECS (°C)	Preservable area ^b (% of preind.)	MDS($L_{\Omega > 3}$) ^c (%/decade)
1.5	74–11	26–80
3.0	73–11	26–79
4.5	73–12	26–78

^a The first emission reductions starting year t_1 for which the Southern Ocean becomes partially undersaturated with respect to aragonite in 2100 ($A_{SO} > 0$). Note that this is an approximation because not all t_1 are simulated, only $t_1 = 2015, 2018, 2020, 2023, \dots, 2045$ (section 2.1).

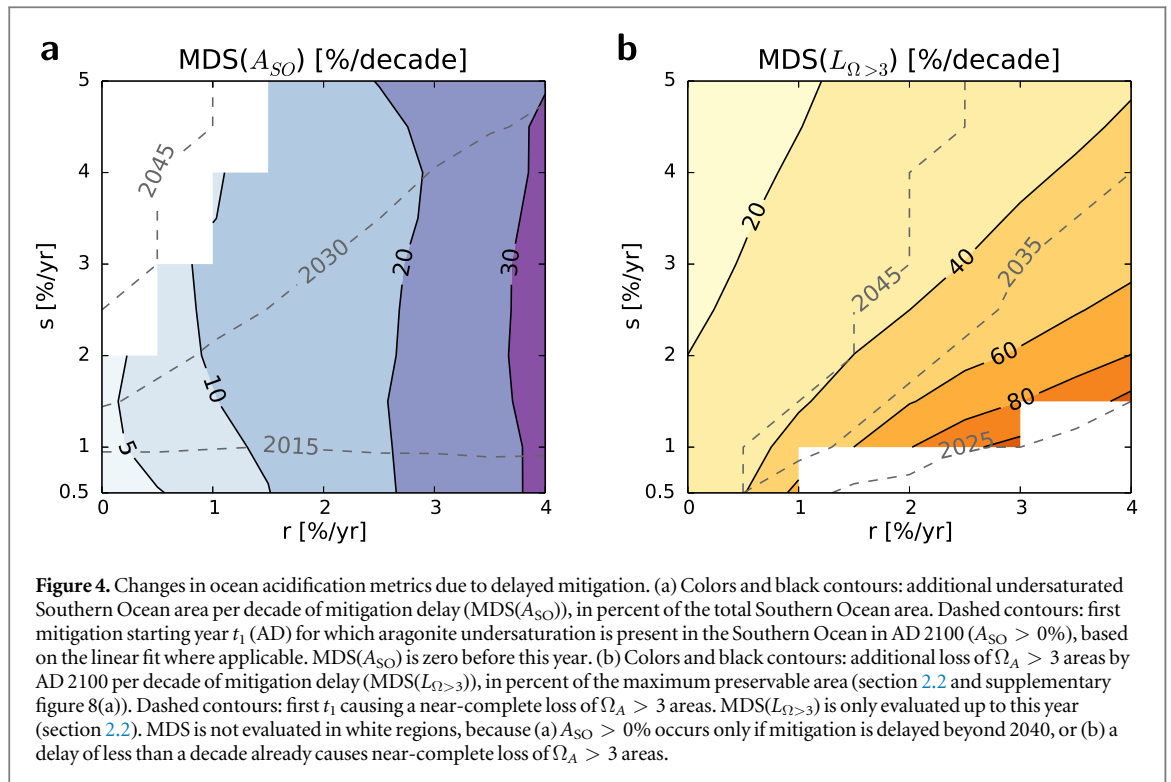
^b This is the fraction of the preindustrial $\Omega_A > 3$ area remaining by 2100 if emission reductions start in 2015, i.e., the maximum preservable area for a given s . It is the baseline for MDS($L_{\Omega > 3}$) (see text).

^c Only fitted for $s = 1$ –5%/yr (see text). The preservable area for $s = 1$ %/yr is roughly 25% of preindustrial.

corresponds to a larger part of the preservable baseline for smaller s . Also note that MDS($L_{\Omega > 3}$) is only defined up to a near-complete loss (< 5% of the preindustrial area remaining, section 2.2). For $s = 0.5$ %/yr, a near-complete loss is imminent for delays of 5–8 years, therefore no decadal MDS fit is obtained in this case. For higher s , a near-complete loss becomes

unavoidable within roughly 1–4 decades of delay. In summary, our model results indicate that the emissions reduction rate s is crucial for the future extent of potential coral reef habitats.

Lastly, we also consider the influence of different emission increase rates r on the MDS estimates for the ocean acidification metrics (figure 4). While MDS (A_{SO}) (colors and solid contours in figure 4(a)) is nearly independent of s , it strongly increases with increasing r . In contrast, the threshold delay for $A_{SO} > 0$ (dashed in figure 4(a)) is influenced by both r and s . This difference can be explained by the fact that Ω_A is mainly driven by atmospheric CO_2 concentrations. The threshold delay depends on absolute concentrations by 2100, which are determined by cumulative CO_2 emissions and uptake, the former depending directly on r and s . On the other hand, MDS (A_{SO}) depends on the change in concentrations with changing t_1 , which is mainly influenced by r in 2100 (s becomes more important on longer time scales). MDS ($L_{\Omega > 3}$) (colors and solid contours in figure 4(b)) increases with decreasing s and increasing r because, by definition, $L_{\Omega > 3}$ is related to both the baseline and its changes (section 2.2). Dashed contours in figure 4(b) indicate peak emission times t_1 causing a near-complete loss of $\Omega_A > 3$ areas. Contours beyond $t_1 = 2045$ are missing, but can be inferred from the MDS: e.g., the MDS($L_{\Omega > 3}$) = 20%/decade contour should roughly correspond to a near-complete loss after five decades of mitigation delay. On a side note, the $t_1 = 2035$ contour nearly coincides with $r = s$, indicating that a near-complete loss becomes unavoidable within less than two decades of delay if the achievable s is smaller than r .



4. Discussion

The MDS(ΔT_{\max}) estimates from the Bern3D-LPX are comparable to earlier estimates from less comprehensive models. Hare and Meinshausen (2006) used a one-dimensional climate model (MAGICC) to evaluate a ‘geophysical warming commitment’, defined as $\Delta T(2100)$ resulting from a business-as-usual emission increase until a sudden emission stop. For this special case described by $s \rightarrow \infty$, they found a decadal increase in this warming commitment by 0.2–0.3 K. This is consistent with our lowest MDS estimates. Friedlingstein *et al* (2011) found a similar decadal increase in an EMIC, but for $s = 3\%/yr$ and $\Delta T(3000)$. Reviewing earlier model studies, Ramanathan (1988) reported a decadal increase in committed equilibrium warming of 0.13–0.5 °C/decade. These somewhat lower estimates are also in agreement with our MDS range, considering that equilibrium warming is smaller than the peak ΔT_{\max} , and that ΔT_{\max} is reached before AD 3000 in most cases (section 2.2, Zickfeld and Herrington 2015). Using the linear relation $\Delta T_{\max} = \beta_T C_\infty$, Allen and Stocker (2014) calculated an MDS of 0.4 °C/decade for a scenario that respects the 2 °C target in case of immediate emission reductions. While we did not simulate this exact scenario, our results for intermediate scenarios are consistent with this analytical estimate. For a better comparison, we estimated MDS analytically for all scenarios using model-diagnosed values for β and historical emissions. These analytical fits are in close agreement with the model results except for high-emission scenarios, where the $\Delta T_{\max}/C_\infty$ relationship

becomes increasingly nonlinear, especially for high ECS. This comparison is presented in the supplementary material.

For the other Earth system variables, we do not find earlier results that are directly comparable to MDSs. Realistic simulation of ocean heat uptake, which is essential for the determination of transient SSLR, requires three-dimensional ocean models. However, Williams *et al* (2012) have shown that, similar to ΔT_{\max} , equilibrium SSLR can be well emulated by the linear relation $SSLR = \beta_{SSLR} C_\infty$. This is also true for the near-equilibrium SSLR simulated by the Bern3D-LPX model, as shown by analytical fits (supplementary section 1). The agreement of simulated and fitted MDS(SSLR) indicates that analytical considerations valid for MDS(ΔT_{\max}) (Allen and Stocker 2014) are also applicable to any other Earth system variable that is linearly related to C_∞ . This includes their finding that ΔT_{\max} increases at the same rate r as C_∞ . Examples for other variables that are near-linearly related to cumulative emissions include changes in ocean surface pH and in the Atlantic meridional overturning circulation (Steinacher and Joos 2015). Because SSLR is mainly driven by temperature changes, the ECS range provides a reasonable estimate for uncertainty in MDS(SSLR), which is supported by the model-data agreement of historical SSLR uncertainty (table 1). However, both ΔT_{\max} and SSLR are also affected by the uncertainty in global carbon uptake, which is described further below. While this increases the total uncertainty of the projected changes, the agreement of β_T and β_{SSLR} ranges with that of other models (supplementary section 1.1)

suggests that the plausible range of temperature and SSLR responses to CO₂ emissions is largely captured by the ECS range in our model.

The total observed global mean sea level rise (GMSLR) in 1971–2010 was 2.5 times as large as observed SSLR over that period (Church *et al* 2013). In the future, this ratio is estimated to increase to roughly 5.5, as Church *et al* (2013) report a 2000 year GMSLR commitment of 2.3 m/°C, opposed to an SSLR commitment of 0.42 m/°C. Multiplying our MDS(SSLR) estimate for an intermediate ECS with this ratio, we get a rough estimate for MDS(GMSLR), amounting to 0.43–1.16 m/decade. This is roughly 20–60 times as fast as the 1971–2010 observed GMSLR of 2.0 cm/decade (Church *et al* 2013). These numbers would be even higher for equilibrium GMSLR, mainly because the meltdown of the Greenland ice sheet takes tens of thousands of years (Church *et al* 2013). More comprehensive models including contributions from ice sheets and glaciers could be employed to better estimate the MDS of GMSLR, for a smaller set of scenario parameters. This MDS may be time-dependent due to nonlinear ice loss effects.

The ocean acidification metrics are much less affected by the ECS uncertainty than the physical variables. The slight differences for different ECSs (table 2) are due to climate-carbon cycle feedbacks (Plattner *et al* 2001, Friedlingstein *et al* 2014), most notably the temperature sensitivity of land and ocean carbon uptake. Not only the temperature sensitivities, but also the total magnitude of land and ocean carbon uptake are subject to considerable model uncertainties (Friedlingstein *et al* 2014). Treatment of these uncertainties would require using an ensemble of different models, or an ensemble of different parameter sets influencing the carbon uptake (Steinacher *et al* 2013). This not feasible here, because the variation of scenario and ECS parameters already requires a large number of model simulations (section 2.1). The land carbon uptake of the Bern3D-LPX model may be too low as indicated by the comparison with historical estimates (section 2.1). This may lead to an overestimation of ocean acidification in the projections. On the other hand, evaluating ocean acidification metrics in AD 2100 underestimates the stress for marine organisms: acidification is strongest after atmospheric CO₂ concentrations peak, which may be before or after 2100 depending on scenario. In addition, marine organisms are not only affected by ocean acidification but also by thermal stress (Pörtner *et al* 2014).

The scenario uncertainty is partly covered by the variation of the policy-relevant parameters r , s , and t_1 . The suite of idealized emission scenarios covers a broad range of cumulative emissions, but for emission path-dependent variables (including our ocean acidification metrics), some uncertainty remains on how results would change under a more gradual transition from emission increase to decrease. This probably does not influence the physical variables notably

(Caldeira and Kasting 1993, Williams *et al* 2012, Zickfeld *et al* 2012), although a slight path-dependence was found for SSLR with more drastic path changes (Zickfeld *et al* 2012). Non-CO₂ forcings are not included in our idealized scenarios, therefore the results of this study only concern mitigation of CO₂ emissions. This may lead to an underestimation of projected ΔT_{\max} (Stocker *et al* 2013) and SSLR, but should only slightly affect the CO₂-driven Ω_A metrics, again via climate-carbon cycle feedbacks.

It is evident that the MDS does not carry the full information on future Earth system changes. In the case of ΔT_{\max} and SSLR, the consequences of adopting a lower reduction rate s are not entirely reflected in the increase in MDS, as the 2015 committed ΔT_{\max} and SSLR also increase markedly. For example, choosing $s = 1\%/yr$ instead of $s = 2\%/yr$ does not only increase MDS(ΔT_{\max}) by 0.11 °C/decade, but additionally increases 2015 committed ΔT_{\max} by 0.76 °C (figure 2(a)). Similarly, while MDS(A_{SO}) is weakly influenced by s , the threshold delay for $A_{SO} > 0$ strongly depends on s . Finally, MDS($L_{\Omega > 3}$) contains information on allowable delays before a near-complete loss of $\Omega_A > 3$ areas, but not on absolute area losses. Overall, the MDS is thus most useful for assessing the choice of the emission reduction starting time t_1 given a reduction rate s that is independently limited, e.g., by economic considerations. In reality, target values for s and t_1 cannot be chosen independently. They are linked both in terms of feasibility, e.g., due to technological advances before t_1 or the lock-in of carbon intensive infrastructure (Jakob *et al* 2012), and in terms of impacts on the future Earth system (this study). Nonetheless, communicating the MDS of relevant Earth system variables, in addition to the classical reporting of current trends and total projected future changes, would permit a more transparent assessment of the Earth system impacts of these choices.

5. Conclusions

Our model results support the analytical finding of Allen and Stocker (2014) that peak committed warming increases much faster than observed warming, at least as long as global emission reductions are delayed. In addition, these results show that delaying emission reductions also increases the committed changes in other Earth system variables rapidly. Like peak temperature, any Earth system variable that is linearly related to cumulative emissions increases at the same relative rate as annual emissions. While emissions continue to increase at the current rate, peak committed temperatures rise 3–7.5 times as fast as 1951–2012 global mean temperatures, and millennial SSLR increases 7–25 times as fast as 1971–2010 SSLR, depending on the rate of emission reductions after emissions peak. For an intermediate ECS, this

corresponds to an absolute MDS of 0.3–0.7 °C/decade for ΔT_{\max} and 8–21 cm/decade for SSLR. In order to better constrain these absolute ranges, the uncertainty associated with ECS should be reduced. Based on a rough estimate, the MDS of total sea level rise is much larger than the MDS of SSLR, and its factor compared to recent rates may also be larger.

Our results further show that ocean acidification metrics by AD 2100 are very sensitive to delays in emission reductions now, especially the loss of surface ocean areas with more than threefold aragonite supersaturation. Depending on the achievable rate of emission reductions, a near-complete loss of such areas by the end of the century becomes unavoidable within a few years or decades of delay.

In view of communicating future climate risks, MDSs are highly informative as they link policy decisions today with long-term consequences in the Earth system. By comparing MDSs with the current trends, the full extent of Earth system changes due to delay in reducing anthropogenic CO₂ emissions becomes evident.

Acknowledgments

We acknowledge financial support by the Swiss National Science Foundation. We thank Gianna Battaglia, Sebastian Lienert, Gian-Kasper Plattner, Raphael Roth and Renato Spahni for discussion and support, as well as two anonymous reviewers for their constructive comments.

References

- Allen M R, Frame D J, Huntingford C, Jones C D, Lowe J A, Meinshausen M and Meinshausen N 2009 Warming caused by cumulative carbon emissions towards the trillionth tonne *Nature* **458** 1163–6
- Allen M R and Stocker T F 2014 Impact of delay in reducing carbon dioxide emissions *Nat. Clim. Change* **4** 23–6
- Archer D *et al* 2009 Atmospheric lifetime of fossil fuel carbon dioxide *Annu. Rev. Earth Planet. Sci.* **37** 117–34
- Boden T A, Marland G and Andres R J 2013 *Global, Regional, and National Fossil-Fuel CO₂ Emissions* Carbon Dioxide Information Analysis Center, Oak Ridge National Laboratory, US Department of Energy, Oak Ridge, Tenn., USA
- Bosetti V, Carraro C, Sgobbi A and Tavoni M 2009 Delayed action and uncertain stabilisation targets, How much will the delay cost? *Clim. Change* **96** 299–312
- Bowerman N H A, Frame D J, Huntingford C, Lowe J A, Smith S M and Allen M R 2013 The role of short-lived climate pollutants in meeting temperature goals *Nat. Clim. Change* **3** 1021–4
- Caldeira K and Kasting J 1993 Insensitivity of global warming potentials to carbon dioxide emission scenarios *Nature* **366** 251–3
- Church J *et al* 2013 Sea level change *Climate Change 2013: The Physical Science Basis. Contribution of Working Group I to the Fifth Assessment Report of the Intergovernmental Panel on Climate Change* ed T F Stocker *et al* (Cambridge: Cambridge University Press) ch 13, pp 1137–1216
- den Elzen M, Meinshausen M and van Vuuren D 2007 Multi-gas emission envelopes to meet greenhouse gas concentration targets: costs versus certainty of limiting temperature increase *Glob. Environ. Change* **17** 260–80
- Dlugokencky E, Tans P and Keeling R 2015 *Atmospheric CO₂ data* NOAA/ESRL (www.esrl.noaa.gov/gmd/ccgg/trends/) and Scripps Institution of Oceanography (scrippsco2.ucsd.edu/)
- Doney S C, Fabry V J, Feely R A and Kleypas J A 2009 Ocean acidification: the other CO₂ problem *Annu. Rev. Mar. Sci.* **1** 169–92
- Etheridge D M, Steele L P, Langenfelds R L, Francey R J, Barnola J-M and Morgan V I 1996 Natural and anthropogenic changes in atmospheric CO₂ over the last 1000 years from air in Antarctic ice and firn *J. Geophys. Res. Atmos.* **101** 4115–28
- Friedlingstein P, Meinshausen M, Arora V K, Jones C D, Anav A, Liddicoat S K and Knutti R 2014 Uncertainties in CMIP5 climate projections due to carbon cycle feedbacks *J. Clim.* **27** 511–26
- Friedlingstein P, Solomon S, Plattner G-K, Knutti R, Ciais P and Raupach M R 2011 Long-term climate implications of twenty-first century options for carbon dioxide emission mitigation *Nat. Clim. Change* **1** 457–61
- Frölicher T L and Paynter D J 2015 Extending the relationship between global warming and cumulative carbon emissions to multi-millennial timescales *Environ. Res. Lett.* **10** 075002
- Hare B and Meinshausen M 2006 How much warming are we committed to and how much can be avoided? *Clim. Change* **75** 111–49
- IPCC 2013 *Climate Change 2013: The Physical Science Basis Contribution of Working Group I to the Fifth Assessment Report of the Intergovernmental Panel on Climate Change* ed T F Stocker (Cambridge: Cambridge University Press)
- Jakob M, Luderer G, Steckel J, Tavoni M and Monjon S 2012 Time to act now? Assessing the costs of delaying climate measures and benefits of early action *Clim. Change* **114** 79–99
- Joos F *et al* 2013 Carbon dioxide and climate impulse response functions for the computation of greenhouse gas metrics: a multi-model analysis *Atmos. Chem. Phys.* **13** 2793–825
- Kleypas J A, McManus J W and Meñez L A B 1999 Environmental limits to coral reef development: where do we draw the line? *Am. Zool.* **39** 146–59
- Luderer G, Pietzcker R C, Bertram C, Kriegler E, Meinshausen M and Edenhofer O 2013 Economic mitigation challenges: how further delay closes the door for achieving climate targets *Environ. Res. Lett.* **8** 034033
- Matthews H D, Gillett N P, Stott P A and Zickfeld K 2009 The proportionality of global warming to cumulative carbon emissions *Nature* **459** 829–32
- Müller S A, Joos F, Edwards N R and Stocker T F 2006 Water mass distribution and ventilation time scales in a cost-efficient, three-dimensional ocean model *J. Clim.* **19** 5479–99
- Orr J *et al* 2005 Anthropogenic ocean acidification over the twenty-first century and its impact on calcifying organisms *Nature* **437** 681–6
- Peters G P, Andrew R M, Boden T, Canadell J G, Ciais P, Le Quere C, Marland G, Raupach M R and Wilson C 2013 The challenge to keep global warming below 2 °C *Nat. Clim. Change* **3** 4–6
- Plattner G-K, Joos F, Stocker T F and Marchal O 2001 Feedback mechanisms and sensitivities of ocean carbon uptake under global warming *Tellus B* **53** 564–92
- Plattner G-K *et al* 2008 Long-term climate commitments projected with climate-carbon cycle models *J. Clim.* **21** 2721–51
- Pörtner H-O, Karl D, Boyd P, Cheung W, Lluch-Cota S, Nojiri Y, Schmidt D and Zavialov P 2014 *Ocean systems Climate Change 2014: Impacts, Adaptation, and Vulnerability. Part A: Global and Sectoral Aspects. Contribution of Working Group II to the Fifth Assessment Report of the Intergovernmental Panel on Climate Change* ed C B Field *et al* (Cambridge: Cambridge University Press) ch 6, pp 411–484
- Ramanathan V 1988 The greenhouse theory of climate change: a test by an inadvertent global experiment *Science* **240** 293–9
- Ritz S P, Stocker T F and Joos F 2011 A coupled dynamical ocean-energy balance atmosphere model for paleoclimate studies *J. Clim.* **24** 349–75

- Rogelj J, Hare W, Lowe J, van Vuuren D P, Riahi K, Matthews B, Hanaoka T, Jiang K and Meinshausen M 2011 Emission pathways consistent with a 2 °C global temperature limit *Nat. Clim. Change* **1** 413–8
- Roth R, Ritz S P and Joos F 2014 Burial-nutrient feedbacks amplify the sensitivity of atmospheric carbon dioxide to changes in organic matter remineralisation *Earth Syst. Dyn.* **5** 321–43
- Siegenthaler U, Monnin E, Kawamura K, Spahni R, Schwander J, Stauffer B, Stocker T F, Barnola J-M and Fischer H 2005 Supporting evidence from the EPICA Dronning Maud Land ice core for atmospheric CO₂ changes during the past millennium *Tellus B* **57** 51–7
- Steinacher M and Joos F 2015 Earth system responses to cumulative carbon emissions *Biogeosci. Discuss.* **12** 9839–77
- Steinacher M, Joos F and Stocker T F 2013 Allowable carbon emissions lowered by multiple climate targets *Nature* **499** 197
- Stocker B D, Roth R, Joos F, Spahni R, Steinacher M, Zaehle S, Bouwman L, Xu-Ri and Prentice I C 2013 Multiple greenhouse-gas feedbacks from the land biosphere under future climate change scenarios *Nat. Clim. Change* **3** 666–72
- Stocker T F 2013 The closing door of climate targets *Science* **339** 280–2
- Tschumi T, Joos F and Parekh P 2008 How important are Southern Hemisphere wind changes for low glacial carbon dioxide? A model study *Paleoceanography* **23** PA4208
- UNESCO 1981 Tenth report of the joint panel on oceanographic tables and standards *Unesco Technical Papers in Marine Science* 36
- Weaver A J, Zickfeld K, Montenegro A and Eby M 2007 Long term climate implications of 2050 emission reduction targets *Geophys. Res. Lett.* **34** L19703
- Williams R G, Goodwin P, Ridgwell A and Woodworth P L 2012 How warming and steric sea level rise relate to cumulative carbon emissions *Geophys. Res. Lett.* **39** L19715
- Zickfeld K, Arora V K and Gillett N P 2012 Is the climate response to CO₂ emissions path dependent? *Geophys. Res. Lett.* **39** L05703
- Zickfeld K and Herrington T 2015 The time lag between a carbon dioxide emission and maximum warming increases with the size of the emission *Environ. Res. Lett.* **10** 031001
- Zickfeld K *et al* 2013 Long-term climate change commitment and reversibility: an EMIC intercomparison *J. Clim.* **26** 5782–809